Low-Energy Ion−Surface Collisions Characterize Alkyl- and Fluoroalkyl-Terminated Self-Assembled Monolayers on Gold

Darrin L. Smith,† Vicki H. Wysocki,*,† Ramon Colorado, Jr.,‡ Olga E. Shmakova,‡ Michael Graupe,‡ and T. Randall Lee‡

Department of Chemistry, University of Arizona, Tucson, Arizona 85721-0041, and Department of Chemistry, University of Houston, Houston, Texas 77204-5003

Received June 29, 2001. In Final Form: February 11, 2002

Self-assembled monolayers (SAMs) formed from alkyl-terminated, CF_3-terminated, CF_3CF_2-terminated, and $C_{10}F_{21}$-terminated alkanethiolates on gold substrates were examined by low-energy (eV) ion−surface collisions to determine the impact of varying the degree of fluorination of the thiolate tail group. The fluorine-terminated SAMs are compared and contrasted to previously examined CF_3-terminated Langmuir−Blodgett films. Polyatomic ($M^{+\bullet}$ for benzene and pyrazine) and atomic ($Mo^{+\bullet}$ and $Cr^{+\bullet}$) ions were collided with the different SAM films at various collision energies (20−70 eV). Data indicate that substitution of CH_3 with CF_3 as the terminal group has a substantial influence on the ion−surface interactions, including energy transfer (fragmentation), electron transfer (neutralization), and atom/group transfer (reaction). However, slight penetration into a depth of the film is apparent and illustrated with the formation of certain ion−surface reaction products and the intensities of those products. This penetration has a noticeable effect on low-energy ion−surface collisions. Also, results for a series of $CF_3(CH_2)_nS$−Au films (where n = 12, 13, 14, 15) illustrate that ion−surface reactions vary with the orientation of the fluorine atoms that are present in the terminal group. The results from collisions of low-energy ions with these relatively well-defined surfaces allow further characterization of the collision events that have the potential to become valuable tools in surface analysis.

Introduction

Organic thin films, for example, self-assembled monolayers (SAMs) and Langmuir−Blodgett (L−B) films, have been used as the basis for nanoscale coatings, advanced lubricant systems, and molecular-based devices.[1−5] Organic thin films are attractive due to the ability to modify the physical and chemical properties of a surface by tailoring the functional groups exposed at an interface. To improve our knowledge of the physical and chemical properties of these organic thin films, surface characterization is usually performed with multiple complementary surface techniques. Some of these current techniques include contact angle measurements, ellipsometry, Fourier transform infrared spectroscopy (FTIR), Raman spectroscopy, scanning tunneling microscopy (STM), and atomic force microscopy (AFM).[6−9] Low-energy ion−surface collisions (≤100 eV) utilizing polyatomic and atomic projectiles could also become a complementary technique from which information is gained about the fundamental physical and chemical properties that are unique to individual SAM films. Low-energy ion−surface collisions contrast the established method of secondary ion mass spectrometry (SIMS), where high-energy (keV) ion collisions with surfaces sputter material from the surface for chemical analysis.[10,11]

Cooks and co-workers and Wysocki and co-workers first reported ion−surface collisions with target surfaces modified with self-assembled monolayers.[12,13] At least four surface-induced processes are observed when SAMs are employed for ion−surface experiments: (i) dissociation of the projectile ion, (ii) reaction between the projectile and atom/groups of the target surface, (iii) neutralization of the projectile ion, and (iv) chemical sputtering of the target surface. (i) Low-energy collisions of polyatomic ions with SAMs transfer a portion of the kinetic energy to internal modes of the polyatomic ions, making the process an alternative activation technique for tandem mass spectrometry (MS/MS) compared to collisions with a gaseous target (collision-induced dissociation, CID).[18,21] Surface-induced dissociation (SID) provides a higher average transfer of kinetic to internal energy (T → V) for polyatomic projectile ions and a relatively narrow distribution (a few eV) of internal energies deposited into the ions when compared to CID.[14−18] The SID method has become valuable in determining the relative dissociation energy

* To whom correspondence should be addressed. Telephone: (520) 621-2628. Fax: (520) 621-8407. E-mail: vwysocki@u.arizona.edu.
† University of Arizona.
‡ University of Houston.

(1) Bonner, T.; Baratoff, A. *Surf. Sci.* **1997**, *377*, 1082−1086.
(2) Bumm, L. A.; Arnold, J. J.; Cygan, M. T.; Dunbar, T. D.; Burgin, T. P.; Jones, L.; Allara, D. L.; Tour, J. M.; Weiss, P. S. *Science* **1996**, *271*, 1705−1707.
(3) Tour, J. M.; Jones, L.; Pearson, D. L.; Lamba, J. J. S.; Burgin, T. P.; Whitesides, G. M.; Allara, D. L.; Parikh, A. N.; Atre, S. V. *J. Am. Chem. Soc.* **1995**, *117*, 9529−9534.
(4) Allara, D. L.; Dunbar, T. D.; Weiss, P. S.; Bumm, L. A.; Cygan, M. T.; Tour, J. M.; Reinerth, W. A.; Yao, Y.; Kozaki, M.; Jones, L. In *Molecular Electronics*: *Science and Technology*; Aviram, A., Ratner, M., Eds.; New York Academy of Sciences: New York, 1998; pp 349−370.
(5) Tamada, K.; Nagasawa, J.; Nakanishi, F.; Abe, K.; Hara, M.; Knoll, W.; Ishida, T.; Fukushima, H.; Miyahita, S.; Usui, T.; Koini, T.; Lee, T. R. *Thin Solid Films* **1998**, *329*, 150−155.
(6) Ulman, A.; Evans, S. D.; Shnidman, Y.; Sharma, R.; Eilers, J. E. *Adv. Colloid Interface Sci.* **1992**, *39*, 175−224.
(7) Wong, S. S.; Takano, H.; Porter, M. D. *Anal. Chem.* **1998**, *70*, 5209−5212.
(8) Pemberton, J. E.; Bryant, M. A.; Sobocinski, R. L.; Joa, S. L. *J. Phys. Chem.* **1992**, *96*, 3776−3782.
(9) Bertilsson, L.; Liedberg, B. *Langmuir* **1993**, *9*, 141−149.
(10) Winograd, N. *Anal. Chem.* **1993**, *65*, A622−A629.
(11) Benninghoven, A.; Hagenhoff, B.; Niehuis, E. *Anal. Chem.* **1993**, *65*, A630−A640.
(12) Winger, B. E.; Julian, R. K.; Cooks, R. G.; Chidsey, C. E. D. *J. Am. Chem. Soc.* **1991**, *113*, 8967−8969.
(13) Wysocki, V. H.; Jones, J. L.; Ding, J. M. *J. Am. Chem. Soc.* **1991**, *113*, 8969−8970.

10.1021/la010998r CCC: $22.00
Published on Web 04/17/2002

requirements and dissociation mechanisms of protonated peptides and small protein ions generated by electrospray ionization (ESI).[14,15,19−23] (ii) Product ions arising from atom/group transfer from the organic film to the projectile ion are sometimes observed, particularly with odd-electron projectiles. These reaction product ions provide the ability to characterize not only the projectile ion but also the chemical composition of the surface. Reaction product ions formed by abstraction of hydrogen, fluorine, chlorine, and C_nH_m from organic thin films with an assortment of atomic and molecular projectile ions have been reported.[24−29] Wysocki and co-workers utilized isotopically labeled L−B films (^{13}C- and ^{2}H-terminated) to demonstrate that ion−surface reactions occur predominantly between the projectile ion and the uppermost portion of organic thin films.[30] Recently, ion−surface reactions utilizing pyrazine projectile ions were used for characterization of CH_3-terminated alkanethiols having odd and even chain lengths.[29] Specifically, odd-numbered chain length films orient on the surface of gold such that the terminal C−C bond is more parallel to the plane of the surface than for even-numbered chain length films. It was determined that this parallel orientation allows, on average, one hydrogen atom on the terminal methyl group for odd numbered chains to be in a more reactive position with incoming pyrazine ions than for even-numbered chain lengths.[29] (iii) Ion collisions with organic thin film surfaces were revealed to enhance detected ion current when compared to collisions with bare metal surfaces.[24,31] A barrier for electron transfer between the bare metal film and the incoming projectile ion is formed, resulting in a reduced amount of neutralized probe ions. However, the film does not act as an insulating layer in which charge accumulation could occur.[32] (iv) Ions from chemical sputtering can also appear and are useful for characterizing the chemical composition of a sample surface. Ionization of the organic thin film has been attributed to a charge exchange mechanism between the projectile ion and the target surface.[33] The degree of sputtering appears to depend on the projectile ion, the chemical composition of the target surface, and the collision energy used. The process of chemical sputtering is not significant for the organic thin films and the projectile ions used in the research presented here. Therefore, we provide no data or discussion related to chemical sputtering for the organic thin films examined in this study.

Self-assembled organic thin films that contain fluorine have proven to be interesting and useful targets for low-energy ion−surface collisions. Energy deposition during a SID experiment depends strongly on the composition of the SAMs on the surface. Fluorinated SAM films yield a "harder" surface compared to hydrocarbon SAM films, resulting in a greater average transfer of kinetic to internal energy.[31,34] Several reports suggest that the increased amount of energy transfer for fluorinated surfaces arises from the effective mass increase and/or additional rigidity of the fluorocarbon chain.[12,31,35−37] In addition, higher ionization energies of fluorinated SAMs allow more of the typical organic ions to survive the collision (decrease in neutralization) when compared to hydrocarbon SAMs.[24,31] These comparisons were derived from analyses of SAMs containing multiple fluorinated carbons ($CF_3(CF_2)_n(CH_2)_2$-SH, n = 7, 9, 11) versus n-alkanethiols on gold.[24,31] Perfluorinated, $CF_3(CH_2)_n$-terminated, and stearate L−B films were previously investigated by Gu et al. who established that the presence of fluorine at the terminus of L−B films controls the ion fragmentation, ion neutralization, and ion−surface reactions occurring during low-energy polyatomic ion collisions.[26] The L−B films were employed because CF_3-terminated alkanethiolates were not available to form SAM films at the time of the study. The present research investigates ion−surface collision processes on the now available CF_3-, CF_3CF_2-, and $C_{10}F_{21}$-terminated SAM surfaces.[38−45] This comparison is important because discrete differences between L−B and SAM films exist that can conceivably influence low-energy ion−surface collision processes. The previously investigated fluorinated L−B films were carboxylic acid molecules transferred to an aluminum substrate[46] by physical

(14) Laskin, J.; Denisov, E.; Futrell, J. *J. Phys. Chem. B* **2001**, *105*, 1895−1900.
(15) Laskin, J.; Denisov, E.; Futrell, J. *J. Am. Chem. Soc.* **2000**, *122*, 9703−9714.
(16) Wysocki, V. H.; Ding, J. M.; Jones, J. L.; Callahan, J. H.; King, F. L. *J. Am. Soc. Mass Spectrom.* **1992**, *3*, 27−32.
(17) Dekrey, M. J.; Kenttamaa, H. I.; Wysocki, V. H.; Cooks, R. G. *Org. Mass Spectrom.* **1986**, *21*, 193−195.
(18) Cooks, R. G.; Ast, T.; Mabud, A. *Int. J. Mass Spectrom. Ion Processes* **1990**, *100*, 209−265.
(19) Gu, C. G.; Somogyi, A.; Wysocki, V. H.; Medzihradszky, K. F. *Anal. Chim. Acta* **1999**, *397*, 247−256.
(20) Dongre, A. R.; Jones, J. L.; Somogyi, A.; Wysocki, V. H. *J. Am. Chem. Soc.* **1996**, *118*, 8365−8374.
(21) Dongre, A. R.; Somogyi, A.; Wysocki, V. H. *J. Mass Spectrom.* **1996**, *31*, 339−350.
(22) Tsaprailis, G.; Nair, H.; Somogyi, A.; Wysocki, V. H.; Zhong, W.; Futrell, J. H.; Summerfield, S. G.; Gaskell, S. J. *J. Am. Chem. Soc.* **1999**, *121*, 5142−5154.
(23) Wysocki, V. H.; Tsaprailis, G.; Smith, L. L.; Breci, L. A. *J. Mass Spectrom.* **2000**, *35*, 1399−1406.
(24) Somogyi, A.; Kane, T. E.; Ding, J. M.; Wysocki, V. H. *J. Am. Chem. Soc.* **1993**, *115*, 5275−5283.
(25) Riederer, D. E.; Cooks, R. G.; Linford, M. R. *J. Mass Spectrom.* **1995**, *30*, 241−246.
(26) Gu, C. G.; Wysocki, V. H.; Harada, A.; Takaya, H.; Kumadaki, I. *J. Am. Chem. Soc.* **1999**, *121*, 10554−10562.
(27) Pradeep, T.; Shen, J. W.; Evans, C.; Cooks, R. G. *Anal. Chem.* **1999**, *71*, 3311−3317.
(28) Pradeep, T.; Evans, C.; Shen, J. W.; Cooks, R. G. *J. Phys. Chem. B* **1999**, *103*, 5304−5310.
(29) Angelico, V. J.; Mitchell, S. A.; Wysocki, V. H. *Anal. Chem.* **2000**, *72*, 2603−2608.
(30) Gu, C. G.; Wysocki, V. H. *J. Am. Chem. Soc.* **1997**, *119*, 12010−12011.
(31) Morris, M. R.; Riederer, D. E.; Winger, B. E.; Cooks, R. G.; Ast, T.; Chidsey, C. E. D. *Int. J. Mass Spectrom. Ion Processes* **1992**, *122*, 181−217.
(32) Kane, T. E.; Wysocki, V. H. *Int. J. Mass Spectrom. Ion Processes* **1994**, *140*, 177−184.
(33) Vincenti, M.; Cooks, R. G. *Org. Mass Spectrom.* **1988**, *23*, 317−326.
(34) Cohen, S. R.; Naaman, R.; Sagiv, J. *Phys. Rev. Lett.* **1987**, *58*, 1208−1211.
(35) Callahan, J. H.; Somogyi, A.; Wysocki, V. H. *Rapid Commun. Mass Spectrom.* **1993**, *7*, 693−699.
(36) Pradeep, T.; Miller, S. A.; Cooks, R. G. *J. Am. Soc. Mass Spectrom.* **1993**, *4*, 769−773.
(37) Burroughs, J. A.; Wainhaus, S. B.; Hanley, L. *J. Phys. Chem.* **1994**, *98*, 10913−10919.
(38) Kim, H. I.; Koini, T.; Lee, T. R.; Perry, S. S. *Langmuir* **1997**, *13*, 7192−7196.
(39) Miura, Y. F.; Takenaga, M.; Koini, T.; Graupe, M.; Garg, N.; Graham, R. L.; Lee, T. R. *Langmuir* **1998**, *14*, 5821−5825.
(40) Houssiau, L.; Graupe, M.; Colorado, R., Jr.; Kim, H. I.; Lee, T. R.; Perry, S. S.; Rabalais, J. W. *J. Chem. Phys.* **1998**, *109*, 9134−9147.
(41) Graupe, M.; Takenaga, M.; Koini, T.; Colorado, R., Jr.; Lee, T. R. *J. Am. Chem. Soc.* **1999**, *121*, 3222−3223.
(42) Graupe, M.; Koini, T.; Wang, V. Y.; Nassif, G. M.; Colorado, R., Jr.; Villazana, R. J.; Dong, H.; Miura, Y. F.; Shmakova, O. E.; Lee, T. R. *J. Fluorine Chem.* **1999**, *93*, 107−115.
(43) Colorado, R., Jr.; Lee, T. R. *J. Phys. Org. Chem.* **2000**, *13*, 796−807.
(44) Fukushima, H.; Seki, S.; Nishikawa, T.; Takiguchi, H.; Tamada, K.; Abe, K.; Colorado, R., Jr.; Graupe, M.; Shmakova, O. E.; Lee, T. R. *J. Phys. Chem. B* **2000**, *104*, 7417−7423.
(45) Colorado, R., Jr.; Graupe, M.; Shmakova, O. E.; Villazana, R. J.; Lee, T. R. In *Interfacial Properties on the Submicron Scale*; Frommer, J. E., Overney, R., Eds.; ACS Symposium Series 781; American Chemical Society: Washington, DC, 2001; pp 276−292.
(46) Nakahama, H.; Miyata, S.; Wang, T. T.; Tasaka, S. *Thin Solid Films* **1986**, *141*, 165−169.

adsorption via dipping procedures[47,48] to form three-layer Y-type films. The present research utilizes alkanethiolates covalently attached to gold substrates (via sulfur−gold bonds) by immersion of a gold substrate into an appropriate thiol solution to form a monomolecular layer.[47,49,50] The amphiphilic molecules of the L−B films are orientated approximately perpendicular to the surface normal,[48] which contrasts the orientation of the fluorocarbon and hydrocarbon SAM chains having a tilt of approximately 17−30° from the surface normal.[51−54]

Previous studies have shown that $CF_3(CH_2)_n$-terminated SAM films are well ordered on the molecular scale and exhibit the same surface packing density as $CH_3(CH_2)_n$-terminated films despite the CF_3 terminal group being markedly larger than CH_3.[38,45] It has also been concluded that the terminal groups of CF_3-terminated chains have the same orientation as CH_3-terminated SAMs for odd and even chain lengths.[40,41,43] The comparison of *n*-alkyl, CF_3-, CF_3CF_2-, and $C_{10}F_{21}$-terminated SAMs presented here demonstrates that the degree of fluorination can exert a profound influence on low-energy ion−surface collision processes. Polyatomic and atomic ion−surface reactions with previously unavailable SAM fluorinated films, for example, CF_3- and CF_3CF_2-terminated, also reveal the depth of sampling into the organic thin film.

Experimental Section

The alkanethiols investigated include alkyl-terminated ($CH_3(CH_2)_{15}SH$), CF_3-terminated ($CF_3(CH_2)_nSH$, where $n = 12$, 13, 14, 15), CF_3CF_2-terminated ($CF_3CF_2(CH_2)_{14}SH$), and $C_{10}F_{21}$-terminated ($CF_3(CF_2)_9(CH_2)_6SH$) thiols. The purity of the fluorinated alkanethiols was checked and verified with gas chromatography−mass spectrometry (GC−MS) (HP 5988A GC/MS). The normal alkanethiol, $CH_3(CH_2)_{15}SH$ (92%), was purchased from Aldrich and used without further purification. The synthesis of the CF_3- and CF_3CF_2-terminated alkanethiols has been reported elsewhere.[42] A similar strategy was used to prepare $CF_3(CF_2)_9(CH_2)_6SH$, which gave the following analytical data. ^{1}H NMR (300 MHz, $CDCl_3$): δ 2.53 (q, $J = 7.2$ Hz, 2 H), 1.97−2.10 (m, 2 H), 1.59−1.72 (m, 4 H), 1.32−1.46 (m, 5 H). ^{13}C NMR (75.5 MHz, $CDCl_3$): δ 110−120 (bm, 10 C), 33.89, 31.01 (t, $^2J_{CF} = 23$ Hz), 29.06, 28.15, 24.69, 20.25. HRMS: calcd for $C_{16}H_{13}F_{21}S$ $(M)^{+\bullet}$, 636.0403; found, 636.0393.

The vapor-deposited gold surfaces were purchased from Evaporated Metal Films (Ithaca, NY). The gold surfaces were formed on a 17 mm × 13 mm × 0.5 mm silica base that was covered with a 5 nm adhesion underlayer of titanium and then 100 nm of vapor-deposited gold. The gold surfaces were UV-cleaned for 15 min (Boekel UV cleaner, model 135500) before being placed in appropriate thiol solutions. Monolayer formation was performed by allowing the freshly UV-cleaned gold surface to react in ∼1 mM ethanolic solution of a particular thiol for 72 h.[55] The ethanolic solutions were prepared in glassware cleaned with piranha solution (H_2SO_4/H_2O_2, in a 1:3 volume ratio). ***Caution***: *piranha solution is highly oxidizing, and extreme care should be used when handling.* The films were then rinsed six times by sonication in ethanol, dried under argon, and immediately inserted into the fast entry lock of the mass spectrometer and placed under vacuum.

A detailed description of the basic SID tandem system with recent modifications has been published elsewhere.[16,29] Briefly, two Extrel quadrupole mass analyzers are arranged in a 90° configuration with an adjustable surface holder bisecting the mass analyzers at a 45° angle. Collision energy is controlled by the potential difference between the surface and the ion source, where mass-selected singly charged ions from the first quadrupole collide into the organic thin film. The products of the collision are then focused into and analyzed by the second quadrupole of the tandem system. The surface holder secures four surfaces, where each surface can be individually placed in the ion beam of the mass spectrometer. All four surfaces can be analyzed under the same experimental conditions. During the measurements, the base pressure of the instrument was 5×10^{-7} Torr. The projectile ions, pyrazine$^{+\bullet}$ (Aldrich 99+%), benzene$^{+\bullet}$ (Aldrich 99+%), and $Mo^{+\bullet}$ and $Cr^{+\bullet}$ (from $Mo(CO)_6$ and $Cr(CO)_6$ (Aldrich 99+%)), were generated by 70 eV electron impact (EI).

Results and Discussion

We first compare the results of ion−surface collision reactions with gold surfaces modified with various hydrocarbon and partially fluorinated alkanethiol SAMs, where the overall chain length was held constant, that is, the hydrocarbon alkanethiol, $CH_3(CH_2)_{15}S-Au$ (**C16F0**); its CF_3-terminated counterpart, $CF_3(CH_2)_{15}S-Au$ (**C16F1**); its CF_3CF_2-terminated counterpart, $CF_3CF_2(CH_2)_{14}S-Au$ (**C16F2**); and its $C_{10}F_{21}$-terminated counterpart, $CF_3(CF_2)_9(CH_2)_6S-Au$ (**C16F10**). This series of surfaces was used to assess the influence of fluorine at the terminal position and underlying $(CF_2)_n$ groups in SAM films on each of the ion−surface collision processes, that is, fragmentation, neutralization, and ion−surface reactions. This comparison was performed with the aforementioned polyatomic and atomic ions at low collision energies (<100 eV). We then compare the results of ion−surface collision reactions for gold surfaces modified with a series of CF_3-terminated alkanethiols, $CF_3(CH_2)_nSH$, where $n = 12$, 13, 14, and 15 (**C13F1**, **C14F1**, **C15F1**, and **C16F1**, respectively) to explore possible differences in ion−surface reactions with respect to odd- and even-numbered chain lengths, given that the orientation of the terminal group in SAMs on gold is known to vary systematically with odd versus even chain lengths (vide supra).

Comparison of SAMs Derived from C16F0, C16F1, C16F2, and C16F10. *Energy Conversion Differences (T → V).* Does the translational energy converted to internal modes of the polyatomic projectile ion depend more on the total chain composition or on the chain terminus of the SAM films? To address this question, MS/MS spectra are compared after collisions of pyrazine (*m*/*z* 80) at 20 eV (Figure 1) and benzene (*m*/*z* 78) at 30 eV (Figure 2) with the SAM films. Changing only the terminal group ($CH_3 \rightarrow CF_3$) at the surface (Figure 1a vs Figure 1b and Figure 2a vs Figure 2b) leads to an enhanced conversion of translational energy into internal energy of the projectile ion (T → V), which is reflected by an increase in the relative abundance of the low mass fragments of the molecular ions, that is, *m*/*z* 26 and 53 for pyrazine and *m*/*z* 26, 27, 39, 50−52, and 63 for benzene. Results for all three fluorinated films (Figures 1b,c,d and 2b,c,d) suggest similar energy deposition and are dramatically different when compared to the hydrocarbon film (Figure 1b,c,d vs Figure 1a and Figure 2b,c,d vs Figure 2a). To approximate the percentage of collision energy deposited into the

(47) Ulman, A. *An introduction to ultrathin organic films*: *from Langmuir−Blodgett to self-assembly*; Academic Press: Boston, 1991.
(48) Petty, M. C. *Langmuir−Blodgett films*: *an introduction*; Cambridge University Press: Cambridge, U.K., 1996.
(49) Nuzzo, R. G.; Zegarski, B. R.; Dubois, L. H. *J. Am. Chem. Soc.* **1987**, *109*, 733−740.
(50) Porter, M. D.; Bright, T. B.; Allara, D. L.; Chidsey, C. E. D. *J. Am. Chem. Soc.* **1987**, *109*, 3559−3568.
(51) Tamada, K.; Ishida, T.; Knoll, W.; Fukushima, H.; Colorado, R., Jr.; Graupe, M.; Shmakova, O. E.; Lee, T. R. *Langmuir* **2001**, *17*, 1913−1921.
(52) Tsao, M. W.; Hoffmann, C. L.; Rabolt, J. F.; Johnson, H. E.; Castner, D. G.; Erdelen, C.; Ringsdorf, H. *Langmuir* **1997**, *13*, 4317−4322.
(53) Laibinis, P. E.; Whitesides, G. M.; Allara, D. L.; Tao, Y. T.; Parikh, A. N.; Nuzzo, R. G. *J. Am. Chem. Soc.* **1991**, *113*, 7152−7167.
(54) Walczak, M. M.; Chung, C. K.; Stole, S. M.; Widrig, C. A.; Porter, M. D. *J. Am. Chem. Soc.* **1991**, *113*, 2370−2378.
(55) Kane, T. E.; Somogyi, A.; Wysocki, V. H. *Org. Mass Spectrom.* **1993**, *28*, 1665−1673.

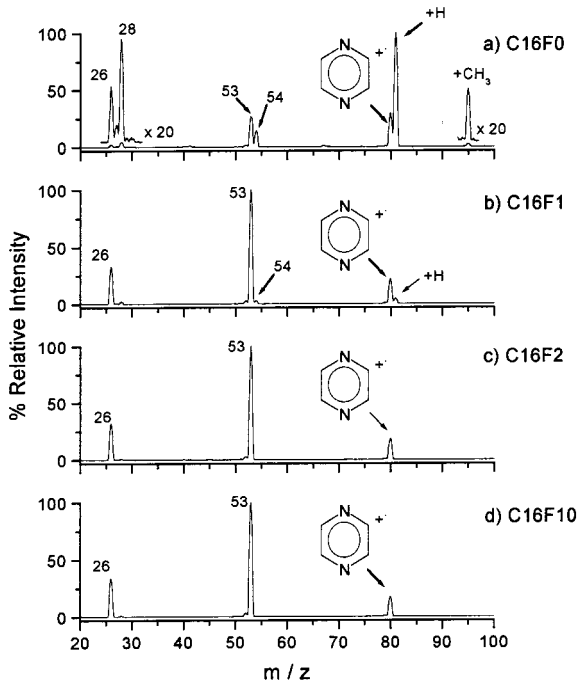

Figure 1. Product spectra formed from collisions between pyrazine at 20 eV kinetic energy and (a) alkyl-terminated (**C16F0**), (b) CF_3-terminated (**C16F1**), (c) CF_3CF_2-terminated (**C16F2**), and (d) $C_{10}F_{21}$-terminated (**C16F10**) SAM films.

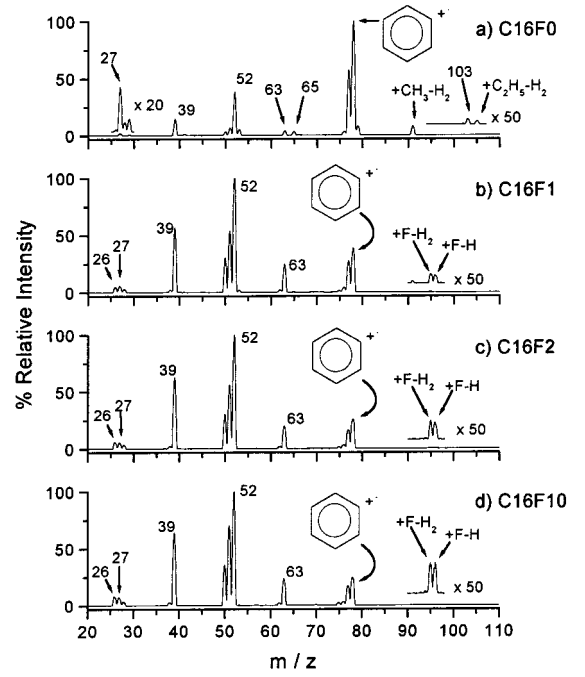

Figure 2. Product spectra formed from collisions between benzene at 30 eV kinetic energy and (a) alkyl-terminated (**C16F0**), (b) CF_3-terminated (**C16F1**), (c) CF_3CF_2-terminated (**C16F2**), and (d) $C_{10}F_{21}$-terminated (**C16F10**) SAM films.

projectile ion, the extended deconvolution method[56] was applied to calculate the internal energy distribution diagrams for benzene with increasing SID collision energies (Figure 3). A variety of methods have been developed that can be used to approximate the amount of internal energy conversion; however, given that the goal of this study was to compare the relative differences in

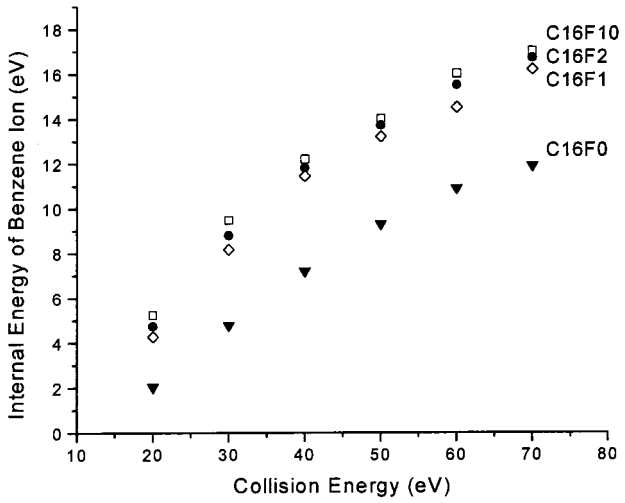

Figure 3. Internal energy conversion into benzene molecular ions plotted versus SID collision energy for **C16F10** (□), **C16F2** (●), **C16F1** (◇), and **C16F0** (▼).

Table 1. Internal Energy Distributions of Benzene Ions at 50 eV

	%T → V			%T → V	
surface	data set A	data set B	surface	data set A	data set B
C16F0	19.0%	18.6%	**C16F2**	–	27.4%
C16F1	26.6%	26.4%	**C16F10**	28.4%	28.0%

energy deposition for various hydrocarbon and fluorocarbon surfaces, alternative estimation methods will not be presented here.[17,37,57,58] Figure 3 demonstrates a significant increase in the conversion of kinetic energy to internal modes of benzene at various collision energies with substitution of the CF_3 group for the CH_3 group. The observed linearity of internal energy as a function of SID collision energy is a reproducible result.[56] However, deviation of linearity could be due to ion−surface reactions and chemical sputtering that are not included in the internal energy estimation. Recently, specific and thorough studies on the linear conversion efficiency in SID have been performed using "cold" electrospray ions.[14,15] The average percentage energy conversion was estimated using internal energy diagrams for each surface at 50 eV (Table 1 displays the %T → V conversion for each film). The first data set (labeled A) was used to probe the influence of the terminal group, and the second (labeled B) was used to highlight the reproducibility of the method and to examine the influence of the underlying CF_2 groups. These data are consistent with reported values for hydrocarbon and fluorocarbon films previously evaluated using the extended deconvolution method.[56] The efficiency for energy conversion for the different SAM surfaces follows the order **C16F10** ≈ **C16F2** ≈ **C16F1** > **C16F0**. The data suggest that a majority of the energy conversion arises from the interaction of the projectile ion with the terminal CF_3 group. However, the further increase in energy conversion with the **C16F2** and **C16F10** SAMs suggests that the underlying $(CF_2)_n$ groups play a measurable role in the energy conversion process. This increase probably originates from an increased effective mass of the target surface.

Ion−Surface Reaction Differences. Do ion−surface reactions vary with changes in the composition of SAM films?

(56) Vekey, K.; Somogyi, A.; Wysocki, V. H. *J. Mass Spectrom.* **1995**, *30*, 212−217.

(57) Beck, R. D.; Rockenberger, J.; Weis, P.; Kappes, M. M. *J. Chem. Phys.* **1996**, *104*, 3638−3650.

(58) Wysocki, V. H.; Kenttamaa, H. I.; Cooks, R. G. *Int. J. Mass Spectrom. Ion Processes* **1987**, *75*, 181−208.

Hydrogen-abstraction products formed upon collisions with pyrazine ions at 20 eV are shown in Figure 1. With the **C16F0** surface (Figure 1a), reactions occur between the molecular pyrazine ions, $M^{+\bullet}$ (*m/z* 80), and available hydrogen atoms of the target film (giving rise to MH^+, *m/z* 81) as well as available methyl groups (giving rise to $[M + CH_3]^+$, *m/z* 95). Also, during the collision, $M^{+\bullet}$ and MH^+ ions gain sufficient internal energy to produce fragment ions at *m/z* 53 and *m/z* 54, corresponding to neutral loss of HCN from the $M^{+\bullet}$ ion and the MH^+ ion, respectively. For the **C16F1** surface (Figure 1b), the reaction with available hydrogen is greatly diminished, and the reaction between the projectile and methyl groups is completely absent. For the **C16F2** and **C16F10** films (Figure 1c,d), peaks corresponding to the addition of hydrogen atoms and methyl groups are extremely small or absent. Therefore, the presence of hydrocarbon contamination from the vacuum chamber appears to be an insignificant factor for the fluorinated films. The mild tendency for hydrogen abstraction from the **C16F1** film is then assumed to arise from exposed hydrogen from the CH_2 group under the CF_3 group. Further evidence to support this conclusion is provided in the discussion section relating to the odd−even CF_3-terminated chains (vide infra). The data presented here also agree with our related pyrazine ion−surface reaction studies of SAMs derived from $CD_3(CH_2)_{19}SH$, $CD_3(CD_2)_{19}SH$, and $CH_3(CH_2)_{19}SH$.[59]

The benzene molecular ion (*m/z* 78) undergoes formal fluorine addition for all the fluorinated films to produce two reaction products, $C_6H_5F^+$ (*m/z* 96) and $C_6H_4F^+$ (*m/z* 95).[24] The fluorinated product ions are illustrated for the **C16F1**, **C16F2**, and **C16F10** films (Figure 2, parts b, c, and d, respectively). The formation of these ions further illustrates that reaction occurs with the uppermost portion of the films, predominantly the terminal group. Benzene (*m/z* 78) can undergo formal addition with available fluorine to produce two reaction products, $C_6H_5F^+$ (*m/z* 96) and $C_6H_4F^+$ (*m/z* 95), which are capable of producing the fragment ions $C_4H_3F^+$, $C_3H_2F^+$, and $C_2H_2F^+$ (*m/z* 70, 57, and 45, respectively).[24] When the integrated normalized peak areas of all fluorinated product ions are divided by the integrated areas of all ions in the spectrum, a normalized ratio of 1.0:0.57:0.24 is generated for $C_{10}F_{21}$-terminated, CF_3CF_2-terminated, and CF_3-terminated surfaces, respectively (i.e., **C16F10** reactivity > **C16F2** > **C16F1**). These data suggest penetration of the benzene molecular ion into the target surface, enabling abstraction of fluorine from underlying (CF_2) groups, which is analogous to the pyrazine molecular ion sampling underlying hydrogen from the **C16F1** SAM (Figure 1b). The presence of the $C_7H_7^+$ ion (*m/z* 91) is also diagnostic, corresponding to formal addition of CH to benzene.[18,24] The *m/z* 91 ion is apparent upon the collision of benzene with the **C16F0** film (Figure 2a), where available methyl groups undergo reaction with benzene ($C_6H_6^{+\bullet} + CH_3 - H_2$). The presence of *m/z* 65, a fragment of the *m/z* 91 reaction ion ($C_7H_7^+ - C_2H_2$), is also observed. These reaction product ions are not observed for the **C16F2** and **C16F10** surfaces (Figure 2, parts c and d, respectively), but the presence of *m/z* 91 was observed for the **C16F1** surface (Figure 2b). The CF_3-terminated film can plausibly give rise to this product ion through two possible pathways: physisorbed hydrocarbon contamination and/or reaction with methylene groups that lie under the terminal group. The lack of hydrogen addition with pyrazine ions and/or methyl addition with benzene ions for the fluorinated films (**C16F2** or **C16F10**) suggests insignificant surface contamination. Therefore, the *m/z* 91 ion probably arises from the film ($C_6H_6^{+\bullet} + CF_3CH_2 - HCF_3$) rather than from contaminants. Further support for this claim is provided in the discussion section regarding SAMs having odd versus even CF_3-terminated chains.

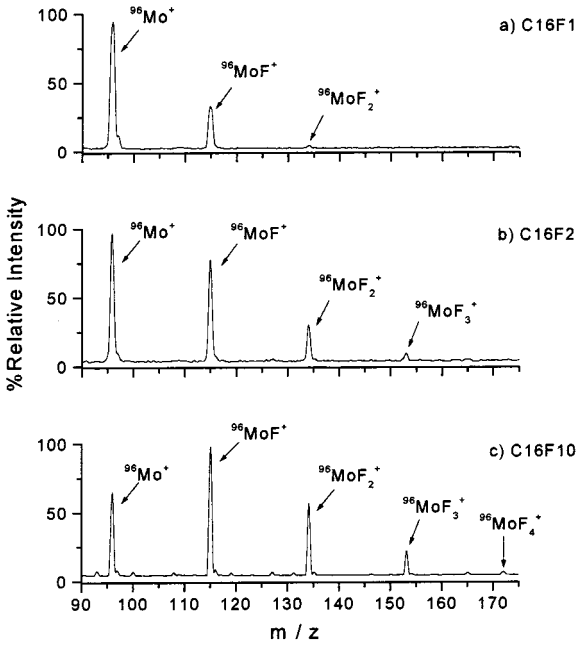

Figure 4. The $^{96}Mo^+$ precursor ion incident at 60 eV was used to abstract fluorine from (a) CF_3-terminated (**C16F1**), (b) CF_3-CF_2-terminated (**C16F2**), and (c) $C_{10}F_{21}$-terminated (**C16F10**) SAM films.

Table 2. Intensity Ratios of $^{96}Mo^{+\bullet}$ Reaction Products at 60 eV

surface	$^{96}Mo^{+\bullet}$	$^{96}MoF^+$	$^{96}MoF_2^{+\bullet}$	$^{96}MoF_3^+$	$^{96}MoF_4^{+\bullet}$
C16F1	100	33	1.9	0.0	0.0
C16F2	100	79	26	5.2	0.0
C16F10	76	100	51	19	2.4

Collisions with atomic projectile ions were employed to provide further evidence for the mechanism proposed for fluorine addition between atomic ions and partially fluorinated SAM films.[60] Cooks and co-workers proposed that fluorine addition occurs from the terminal CF_3 group and underlying CF_2 groups. They suggested that the endothermic abstraction step is probable due to (i) energy release from C=C bond formation between two carbon atoms after fluorine abstraction from each carbon of the CF_3CF_2 terminal group and (ii) depth of penetration into the film, which allows the underlying CF_2 groups to undergo reaction. Fluorine abstraction with $^{96}Mo^{+\bullet}$ precursor ions incident at 60 eV on the partially fluorinated films is shown in Figure 4 with intensity ratios presented in Table 2. The reaction with the CF_3-terminated SAM (Figure 4a) can only involve the interaction of the atomic ion with the fluorine atoms in the terminal CF_3 group. The observed increase in fluorine abstraction with the CF_3CF_2- and $C_{10}F_{21}$-terminated SAMs (Figure 4b,c) suggests that additional abstraction occurs from underlying CF_2 groups. These data are consistent with previous work involving fluorinated SAMs and CF_3-terminated and perfluorinated L−B films.[26,60] The novel aspect of the present comparison lies with the data from the CF_3CF_2-terminated SAMs. If fluorine abstraction occurs only with the first two terminal fluorinated carbon atoms, then

(59) Angelico, V. A.; Dube, C. A.; Wysocki, V. H. To be published.

(60) Pradeep, T.; Riederer, D. E.; Hoke, S. H.; Ast, T.; Cooks, R. G.; Linford, M. R. *J. Am. Chem. Soc.* **1994**, *116*, 8658−8665.

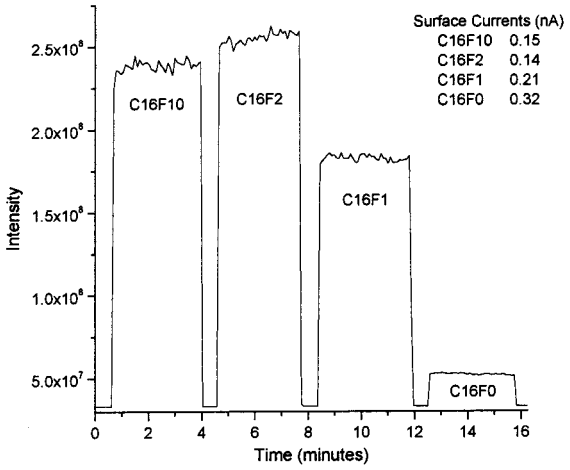

Figure 5. The total scattered-ion current (TIC) measured at the detector of the SID instrument for pyrazine at 20 eV for $C_{10}F_{21}$-terminated (**C16F10**), CF_3CF_2-terminated (**C16F2**), CF_3-terminated (**C16F1**), and alkyl-terminated (**C16F0**) SAM films.

Table 3. Intensity Ratios of $^{52}Cr^{+\bullet}$ Reaction Products at 60 eV

surface	$^{52}Cr^{+\bullet}$	$^{52}CrF^{+}$	$^{52}CrF_2^{+\bullet}$
C16F1	100	14	0.0
C16F2	100	30	0.7
C16F10	100	48	2.5

spectra resulting from collisions between $^{96}Mo^{+\bullet}$ and CF_3-CF_2- and $C_{10}F_{21}$-terminated SAMs should appear similar. However, the intensity ratios are quite distinct (**C16F10** > **C16F2** > **C16F1**), implying that atomic ions penetrate deeper than two atomic layers into the SAM films to abstract fluorine atoms during the collision event. Table 3 shows that a similar trend was monitored by a 60 eV collision of $^{52}Cr^{+\bullet}$ ions (spectra not shown) and the resulting intensity ratios of $Cr^{+\bullet}/CrF^{+}/CrF_2^{+\bullet}$ for the different fluorinated SAMs. These data collectively support the penetration of atomic ions into a few atomic layers of the surface past the first two terminal carbon atoms.[40]

Electron-Transfer Differences. Is electron transfer from the film to the projectile ion predominantly influenced by the composition of the terminal group of SAMs, or does the underlying chain play a strong role? The extent of neutralization of pyrazine molecular ions incident at 20 eV on **C16F0**, **C16F1**, **C16F2**, and **C16F10** surfaces is presented in Figure 5. The total scattered-ion current (TIC) reflects the total number of ions that are detected at the electron multiplier after surviving collisions with the modified surface. The total surviving ions include the precursor, fragment, and reaction ions, that is, all the ions that appear in Figure 1. The baseline in Figure 5 was attained when the EI source filaments were turned off. The TIC plot shows that the partially fluorinated films give less neutralization than the purely hydrocarbon film. The current values, **C16F0** = 0.32 nA, **C16F1** = 0.21 nA, **C16F2** = 0.14 nA, and **C16F10** = 0.15 nA (displayed in the inset of Figure 5), were measured with a picoamperemeter at each of the target surfaces during the collision. Low ion signal measured at the electron multiplier corresponds to enhanced electron transfer, that is, elevated current at the target surface (thus enhanced neutralization, and vice versa). The trend for the current measurements is consistent with the relative total scattered-ion currents shown in Figure 5. This trend was also apparent with collisions of benzene at 30 eV (TIC not shown). The current values measured with benzene for the **C16F0**, **C16F1**, **C16F2**, and **C16F10** SAMs were 0.31, 0.23, 0.12, and 0.11 nA, respectively. For the CF_3-terminated SAM, it appears that a portion of the polyatomic ions penetrate beneath the terminal group, which allows access to the underlying CH_2 groups (lower ionization energy). This small penetration allows a fraction of the ions to experience electron transfer via a pathway distinct from that of the **C16F2** and **C16F10** SAMs. A detailed discussion regarding the neutralization of methyl cations with fluorinated SAM films is forthcoming.[61] Overall, the efficiency of electron transfer to the pyrazine and benzene ions follows the order **C16F0** > **C16F1** > **C16F10** ≥ **C16F2**. These results contrast the results for the previously investigated L−B films, where electron-transfer efficiency followed the order stearate > CF_3-terminated ≈ perfluorinated, that is, CF_3-terminated and perfluorinated films gave more similar values for neutralization.[26] Differences in the observed trends can perhaps be attributed to the enhanced conformational order of SAM films versus L−B films and/or the greater tilt angle for SAM films versus L−B films where CH_2 is exposed in the CF_3-terminated SAM film but not with the L−B film.

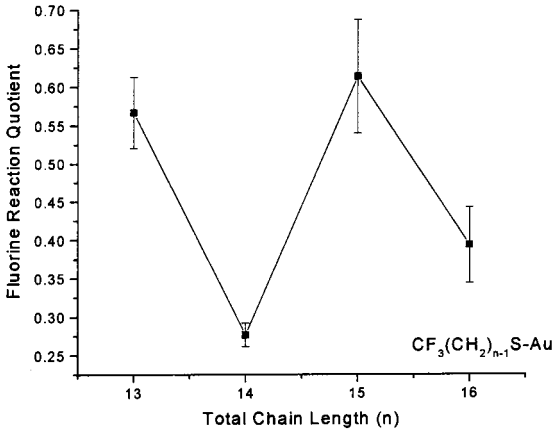

Figure 6. Fluorine addition with benzene at 30 eV incident on CF_3-terminated SAM films on Au. Large quotient values indicate enhanced fluorine abstraction.

Comparison of SAMs Derived from C13F1, C14F1, C15F1, and C16F1. Ion−surface collision data for even- and odd-numbered CF_3-terminated chains were used to examine the orientation differences of the terminal group. The odd−even orientation effect for the CF_3 terminal functional groups relative to the surface has been shown by previous studies.[39−41,43] As mentioned above, benzene (*m/z* 78) can undergo formal addition with available fluorine to produce two reaction products, $C_6H_5F^+$ (*m/z* 96) and $C_6H_4F^+$ (*m/z* 95), which are capable of producing the fragment ions $C_4H_3F^+$, $C_3H_2F^+$, and $C_2H_2F^+$ (*m/z* 70, 57, and 45, respectively).[24] A fluorine reaction quotient for a given chain length can be generated by summing the integrated normalized peak areas of fluorine reaction ions divided by the integrated areas of all ions in the spectrum. The results from these ion−surface reactions are shown in Figure 6 as a plot of the fluorine reaction quotient [(96 + 95 + 70 + 57 + 45)/(total peak area)] versus total carbon chain length. Each data point represents an average of measurements from three independent surfaces prepared at different times and measured in the SID instrument. The standard deviation error bars determined for each sample can be attributed to minor drifts in instrumental conditions as well as minor variations in the quality of the substrates and the films. The magnitude of fluorine

(61) Somogyi, A.; Smith, D. L.; Wysocki, V. H.; Colorado, R., Jr.; Lee, T. R. *J. Am. Soc. Mass Spectrom.*, to be submitted.

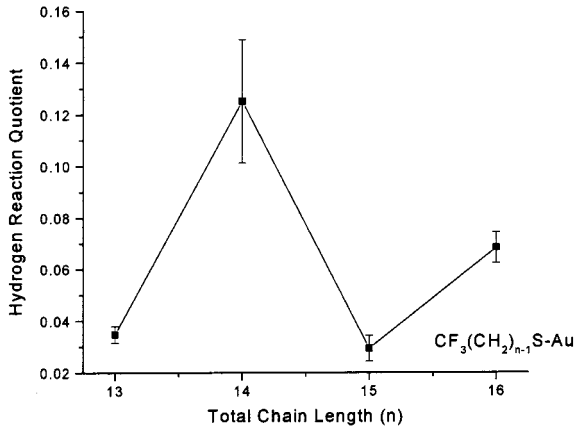

Figure 7. Hydrogen addition with pyrazine at 20 eV incident on CF_3-terminated SAM films on Au. Large quotient values indicate enhanced hydrogen abstraction.

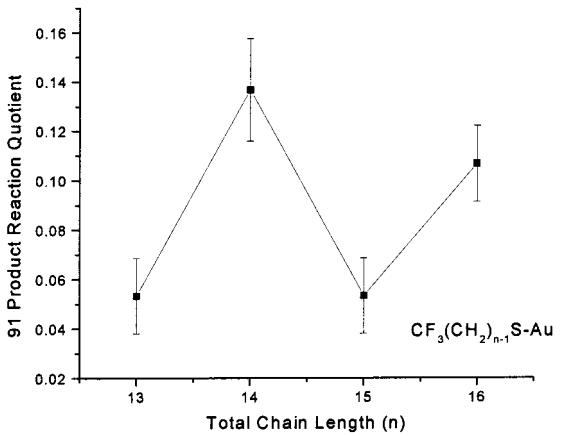

Figure 8. Methyl addition with benzene at 30 eV incident on CF_3-terminated SAM films on Au. Large quotient values indicate enhanced methyl abstraction.

abstraction is greater for odd-numbered chains than for even-numbered chains. This difference can be rationalized on the basis of a model where one fluorine atom of odd-numbered chains extends, on average, substantially above the plane defined by the outermost carbon atom. For even-numbered chains, however, all three fluorine atoms lie slightly above the plane defined by the outermost carbon atom. In the former case, the exposed fluorine atom would appear to be relatively accessible to abstraction. This interpretation is consistent with the suggested orientation of the terminal CF_3 groups in these SAMs[39−41,43] and also parallels the data previously reported for ion−surface reactions involving CH_3-terminated SAMs.[29]

A plot of hydrogen abstraction with pyrazine molecular ions versus chain length showed a similar but reversed trend (Figure 7). The reaction of pyrazine with hydrogen, along with the molecular and reaction fragments, was briefly described above. A hydrogen reaction quotient $[(MH^+ + (MH - HCN)^+)/(M^{+\bullet} + (M - HCN)^{+\bullet})]$ or in terms of *m/z* values [((81) + (54))/((80) + (53))] can also be calculated by using the integrated normalized peak areas of the corresponding ions. Again, each data point represents an average of measurements from three independent surfaces with experimentally determined standard deviation error bars. Moreover, as discussed above, physisorbed hydrocarbon contamination is not significant enough to account for any substantial H-addition. Any contamination that is present should be roughly constant due to the similarities of the CF_3-terminated films; therefore, the present variation of hydrogen abstraction with chain length suggests that the hydrogen originates from the chain rather than from contaminants. The results are quite surprising given the nearly perpendicular orientation of the terminal CH_2-CF_3 bond in the even-numbered chains, which would be expected to inhibit access to the hydrogen atoms of the β-CH_2 group. In contrast, the hydrogen atoms of the β-CH_2 group in odd-numbered chains should be relatively available for abstraction.[62]

Similarly, the *m/z* 91 ion previously observed in the reaction between benzene ions and the **C16F1** surface (Figure 2b) was also observed in the product spectra for all of the CF_3-terminated SAMs, that is, **C13F1**, **C14F1**, **C15F1**, and **C16F1**. We argued above that this product ion arises from the reaction between the benzene ion and the film ($C_6H_6^{+\bullet} + CF_3CH_2 - HCF_3$). In this model, the benzene ion appears to interact directly with the carbon atom of the β-CH_2 group (i.e., the carbon atom attached to the CF_3 group). Although we have yet to unambiguously identify the source of the *m/z* 91 ion, we can tentatively assign it as a reaction ion ($C_7H_7^+$), which is known to be stable and is known to undergo fragmentation to generate a *m/z* 65 ion.[18,24] A *m/z* 91 ion reaction quotient is derived by summing the integrated normalized peak areas of the *m/z* 91 ion and its fragment *m/z* 65 ion divided by the area of the total ions in the spectrum for an individual chain length. From these manipulations, we find that the integrated areas for the *m/z* 91 ion and its fragment *m/z* 65 ion are greater for the even-numbered chain lengths compared to odd-numbered chain lengths (see Figure 8). Again, the enhanced reactivity of the even-numbered chains is surprising given that the β-carbon atoms in these films are likely to be sterically shielded relative to the β-carbon atoms in odd-numbered chains.[39−41,43,62] We note also that the chain-length-dependent formation of these ions again indicates that they are derived from the films rather than from contaminants.

We are left to rationalize the surprisingly enhanced reactivity of the CF_3-terminated SAMs having even-numbered chain lengths. Enhancements in both the addition of hydrogen to pyrazine ions and the formal addition of CH to benzene ions can be argued to result from the even-numbered chains possessing more defects than those having odd-numbered chains. The purity of the alkanethiols was checked and verified with GC−MS, and no interfering contaminations appear to be present. Defect sites present could be a result of multiple phase boundaries formed between ordered SAM domains or disruption at the interface of the even-numbered chain during the collision. These defect sites would permit enhanced access of probe ions into the even-chain-length films for reaction of exposed chain atoms. Studies utilizing CF_3-terminated thiols having specific deuterium labeling (currently not available) should help to clarify these observed reaction pathways.

Conclusions

With the synthesis of new alkanethiols that contain various functional groups, model target surfaces can be constructed to gain an increasing amount of knowledge regarding ion−surface collision processes with self-assembled monolayer films. The resulting information is vital to the development of ion−surface collisions as a surface analytical tool that supplies data regarding organic thin films in terms of exposed atom/group composition, electron transfer in the gas phase, and conversion of kinetic energy to internal energy for the fragmentation of

(62) Shon, Y.-S.; Lee, S.; Colorado, R., Jr.; Perry, S. S.; Lee, T. R. *J. Am. Chem. Soc.* **2000**, *122*, 7556−7563.

projectile ions. From examining results from low-energy ion−surface collisions with various fluorinated SAM surfaces, we have found that the effective mass of the terminal group is the most direct contributor to the extent of translational energy converted to internal energy for polyatomic projectile ions. In the case of SAM films, the underlying groups also play a measurable role in this process. Electron transfer from the surface and through the organic film is predominantly influenced by the nature of the terminal group, that is, CH_3 versus CF_3. However, polyatomic ions penetrate into a depth of the film and clearly indicate differences in electron transfer between CF_3-terminated films and CF_3CF_2- and $C_{10}F_{21}$-terminated films. The nature of the terminal group is also the predominant factor in the chemical transformations occurring during the ion−surface collisions. Slight penetration also influences the ion−surface reactions; therefore, these reactive collisions are sensitive to changes in the exposed atoms or groups in the uppermost atomic layers of the interface. Ion−surface reactions can also detect differences in SAM films having terminal groups with identical chemical composition but differing bulk structure, as observed for CF_3-terminated films having odd-numbered versus even-numbered chain lengths.

Acknowledgment. The $Mo(CO)_6$ is an appreciated gift from Dr. Dennis Lichtenberger at the University of Arizona. Financial support for this research by the National Science Foundation is gratefully acknowledged (Grants CHE-9224719 (V.H.W.) and DMR-9700662 (T.R.L.)).

LA010998R